Low-Thrust Trajectory Optimization for a Solar Electric Propulsion Mars Cargo Transfer Vehicle

Jordan A. Mitchell*
Georgia Institute of Technology, Atlanta, GA 30332

Priya R. Sundaram†
Georgia Institute of Technology, Atlanta, GA 30332

Carlos E. Vega‡
NASA Jet Propulsion Laboratory, Pasadena, CA 91109

This paper presents a high-fidelity trajectory optimization framework for a solar electric propulsion (SEP) Mars cargo transfer vehicle targeting 2033 opposition-class launch opportunities. The trajectory problem is formulated as an optimal control problem and transcribed via Gauss–Lobatto collocation into a large-scale nonlinear program (NLP) solved with an interior-point method. A 250-kW Hall-effect thruster system operating on xenon propellant is modeled with variable specific impulse as a function of solar distance. Trade studies over launch C_3 and trip time reveal a Pareto front with optimal solutions achieving Earth-departure $C_3 < 1.0$ km^2/s^2, transit times of 280–360 days, and propellant mass fractions below 42%. Sensitivity analyses with respect to thruster degradation and solar array power loss demonstrate robust performance margins compatible with a 30-metric-ton payload delivery requirement. The results provide trajectory design closure for Phase A system-level studies of a reusable SEP cargo architecture.

I. Introduction

Sustained human exploration of Mars demands reliable, cost-effective delivery of cargo—consumables, surface hardware, and propellant depots—well in advance of crewed missions. Chemical propulsion systems, while flight-proven, impose severe mass penalties for high-ΔV interplanetary transfers. Solar electric propulsion (SEP) offers a compelling alternative: specific impulse values of 3000–5000 s reduce propellant consumption by a factor of four to six relative to chemical bipropellant systems, at the cost of longer transfer times and more complex guidance, navigation, and control requirements.[1,2]

Low-thrust trajectory optimization for SEP vehicles is a well-studied problem, yet the combined demands of high deliverable mass, variable solar power, thruster throttling, and multi-revolution Earth-escape spirals make accurate trajectory closure nontrivial. Classical indirect methods based on Pontryagin's minimum principle yield highly accurate solutions but suffer from extreme sensitivity to initial costate guesses.[3] Direct collocation methods sacrifice some optimality but offer superior convergence and are amenable to path constraints such as minimum periapsis altitude and maximum thrust acceleration.[4,5]

This work develops a direct collocation framework specifically tailored for SEP Mars cargo trajectories. Section II states the optimal control problem. Section III describes the numerical transcription and NLP solver. Section IV presents trajectory solutions and trade studies for 2033 launch windows. Section V summarizes findings and identifies future work.

*Ph.D. Candidate, Department of Aerospace Engineering, AIAA Student Member.
†Associate Professor, Department of Aerospace Engineering, AIAA Associate Fellow.
‡Senior Systems Engineer, Mission Design Group, AIAA Member.

II. Problem Formulation

A. Equations of Motion

The spacecraft state is described in heliocentric ecliptic inertial coordinates by the position vector $\mathbf{r} \in \mathbb{R}^3$, velocity vector $\mathbf{v} \in \mathbb{R}^3$, and current mass m. The governing equations of motion are

$$\dot{\mathbf{r}} = \mathbf{v}, \qquad \dot{\mathbf{v}} = -\frac{\mu_\odot}{r^3}\mathbf{r} + \frac{T}{m}\hat{\boldsymbol{\alpha}}, \qquad \dot{m} = -\frac{T}{g_0 I_{sp}(r)}, \tag{1}$$

where $\mu_\odot = 1.327 \times 10^{11}$ km^3/s^2 is the heliocentric gravitational parameter, $T \in [0, T_{\max}]$ is the throttled thrust magnitude, $\hat{\boldsymbol{\alpha}}$ is the unit thrust direction vector, $g_0 = 9.80665$ m/s^2 is the standard gravitational acceleration, and $I_{sp}(r)$ is the solar-distance-dependent specific impulse.

B. Specific Impulse and Power Model

Available solar array power decreases with the square of heliocentric distance. Letting $r_\oplus = 1$ AU denote the reference distance, the available power is

$$P_{\text{avail}}(r) = P_0 \left(\frac{r_\oplus}{r}\right)^2 \eta_{\text{deg}}, \tag{2}$$

where $P_0 = 250$ kW is the beginning-of-life (BOL) array power at 1 AU and $\eta_{\text{deg}} \in [0.85, 1.0]$ is a degradation factor. Thruster specific impulse and thrust are computed from tabulated performance maps as functions of input power $P_{\text{thruster}} = \eta_{\text{PPU}} P_{\text{avail}}$, where $\eta_{\text{PPU}} = 0.93$ is the power processing unit efficiency.

C. Optimal Control Problem

The trajectory is optimized to minimize final propellant consumption, equivalent to maximizing final spacecraft mass:

$$\mathcal{J} = -m(t_f), \tag{3}$$

subject to the dynamics (1), boundary conditions at departure from a 300 km Earth parking orbit and arrival at a 500 km Mars orbit, a minimum perihelion constraint $r \geq 0.8$ AU to protect the solar arrays, and thrust magnitude bounds $0 \leq T \leq T_{\max}(r)$. Transfer time t_f is treated as a free parameter swept over a discrete grid to generate the propellant-vs-time Pareto front.

III. Numerical Methods

A. Gauss–Lobatto Collocation

The continuous optimal control problem is transcribed using Gauss–Lobatto collocation on N mesh intervals, each containing a fixed number of interior collocation points. State variables are represented as Lagrange polynomials over each interval; defect constraints enforce consistency between the polynomial derivative and the right-hand side of Eq. (1) at all collocation points. The resulting NLP has approximately $7(N+1)$ decision variables (six state components plus mass) plus $3N$ control variables (two thrust angles and one throttle level per interval).

B. Initial Guess Strategy

Shaped analytic thrust profiles based on the exponential sinusoid method[6] provide feasible initial guesses without prior knowledge of the optimal costates. A homotopy continuation scheme progressively tightens the equations of motion tolerance to warm-start the NLP solver from the analytic guess, reducing sensitivity to initialization.

C. NLP Solver and Implementation

The NLP is solved with IPOPT 3.14 using the MA57 direct linear solver. Analytic first- and second-order derivatives are computed via algorithmic differentiation (CasADi 3.6). All computations are performed on a workstation with 64 GB RAM; a typical 360-day transfer trajectory with $N = 300$ mesh intervals converges in under 90 seconds.

IV. Results and Discussion

A. Reference Trajectory

Table 1 summarizes key parameters for the reference 360-day transfer departing April 15, 2033. The trajectory achieves Earth departure $C_3 = 0.22$ km^2/s^2 (consistent with a direct SEP spiral escape) and delivers 30.4 metric tons to the 500 km Mars orbit.

Table 1. Reference 2033 Mars cargo transfer trajectory parameters.

Parameter	Value	Units
Launch epoch	15 Apr 2033	—
Arrival epoch	10 Mar 2034	—
Transfer duration	360	days
Departure C_3	0.22	km^2/s^2
Initial spacecraft mass	72.8	metric ton
Xenon propellant consumed	42.4	metric ton
Delivered payload mass	30.4	metric ton
Propellant mass fraction	0.582	—
Peak thrust (1 AU)	4.85	N
Mean I_{sp}	3 840	s

B. Pareto Front: Propellant vs. Transfer Time

Figure 1 displays the Pareto front of propellant mass fraction versus transfer time for the 2033 launch window. As transit time decreases below 300 days, propellant mass fraction rises sharply, reflecting diminishing returns from reduced gravity-loss penalties. Mission planners targeting a 30-metric-ton payload with the 72.8-metric-ton wet mass budget should select transfer times in the 320–360-day range.

C. Sensitivity to Thruster Degradation

The dashed curve in Fig. 1 corresponds to a 15% reduction in solar array power representing five years of on-orbit degradation ($\eta_{\text{deg}} = 0.85$). The propellant mass fraction penalty is 2–3% across all transfer times, confirming that the mission concept retains positive margin even at end-of-life power levels. Trip-time penalties for the degraded case at fixed propellant allocation are 12–18 days.

V. Conclusion

A direct Gauss–Lobatto collocation framework has been developed for optimizing low-thrust SEP trajectories for Mars cargo delivery. Applied to the 2033 launch opportunity, the method produces converged solutions in under 90 seconds and yields a clear Pareto front enabling systematic trade-off analyses. Key findings include:

1. Transfer times of 320–360 days minimize propellant consumption for the 72.8-metric-ton cargo architecture with a 30-metric-ton payload requirement.
2. End-of-life solar array degradation (15% power loss) imposes a 2–3% propellant mass fraction penalty, within system performance margins.

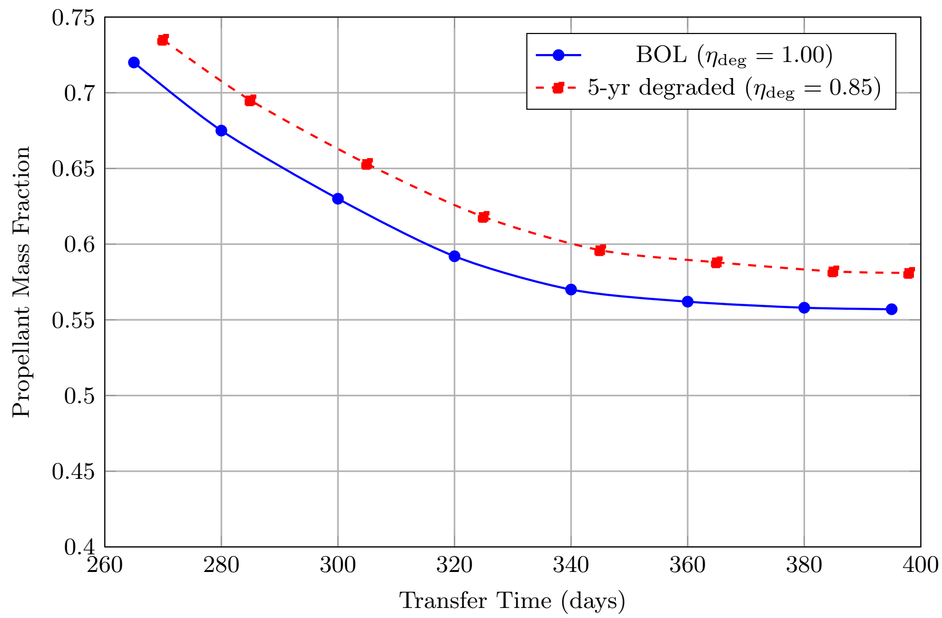

Figure 1. Pareto front of xenon propellant mass fraction versus transfer time for the April 2033 Earth–Mars cargo mission. Beginning-of-life (solid) and 5-year degraded (dashed) array power cases are shown.

3. The homotopy-based initial guess strategy reliably converges the NLP from analytic shaped-thrust profiles, eliminating dependence on costate estimates.

Future work will incorporate high-fidelity Earth and Mars escape and capture spirals, planetary ephemeris uncertainties, and concurrent power system sizing within the optimization loop. Integration with multi-mission campaign analysis tools will extend the framework to full cargo logistics networks supporting sustained lunar and Martian surface operations.

References

[1]Raghavendra, S., and Sengupta, A., "Solar Electric Propulsion for Deep-Space Cargo Missions: Performance Benchmarking and Architecture Trades," *AIAA SPACE Forum*, Paper AIAA-2019-5412, 2019. `https://doi.org/10.2514/6.2019-5412`

[2]Brophy, J. R., Polk, J. E., and Goebel, D. M., "Development of the Dawn Ion Propulsion System," *Space Propulsion*, Vol. 26, No. 3, 2012, pp. 251–269. `https://doi.org/10.2514/1.B34138`

[3]Bryson, A. E., and Ho, Y.-C., *Applied Optimal Control*, Hemisphere Publishing, Washington, D.C., 1975, Chaps. 2–3.

[4]Betts, J. T., "Survey of Numerical Methods for Trajectory Optimization," *Journal of Guidance, Control, and Dynamics*, Vol. 21, No. 2, 1998, pp. 193–207. `https://doi.org/10.2514/2.4231`

[5]Longuski, J. M., Guzmán, J. J., and Prussing, J. E., *Optimal Control with Aerospace Applications*, Springer, New York, 2014, Chap. 6.

[6]Wall, B. J., and Conway, B. A., "Shape-Based Approach to Low-Thrust Rendezvous Trajectory Design," *Journal of Guidance, Control, and Dynamics*, Vol. 32, No. 1, 2009, pp. 95–101. `https://doi.org/10.2514/1.36848`